

Chapter 20

Dynamic High-Temperature Tensile Characterization of an Iridium Alloy

Bo Song, Kevin Nelson, Ronald Lipinski, John Bignell, G.B. Ulrich, and E.P. George

Abstract Iridium alloys have been utilized as structural materials for certain high-temperature applications due to their superior strength and ductility at elevated temperatures. In some applications where the iridium alloys are subjected to high-temperature and high-speed impact simultaneously, the high-temperature high-strain-rate mechanical properties of the iridium alloys must be fully characterized to understand the mechanical response of the components in these severe applications. In this study, the room-temperature Kolsky tension bar was modified to characterize a DOP-26 iridium alloy in tension at elevated strain rates and temperatures. The modifications include (1) a unique cooling system to cool down the bars while the specimen was heated to high temperatures with an induction heater; (2) a small-force pre-tension system to compensate for the effect of thermal expansion in the high-temperature tensile specimen; (3) a laser system to directly measure the displacements at both ends of the tensile specimen independently; and (4) a pair of high-sensitivity semiconductor strain gages to measure the weak transmitted force. The dynamic high-temperature tensile stress–strain curves of the iridium alloy were experimentally obtained with the modified high-temperature Kolsky tension bar techniques at two different strain rates (~ 1000 and 3000 s^{-1}) and temperatures (~ 750 and $1030 \text{ }^\circ\text{C}$).

Keywords Kolsky bar • High temperature • Dynamic tension • Iridium alloy • Stress–strain response

20.1 Introduction

Iridium alloys possess unique property combinations of high melting temperature, high-temperature strength and ductility, and excellent oxidation and corrosion resistance [1–5], making them ideal for specialized applications. In these applications, the high-temperature impact response of the material must be fully understood in order to verify that the component safety envelope is sufficient. High-strain-rate and high-temperature stress–strain tensile data are thus needed to develop strain-rate and temperature dependent material models for safety analysis. The dynamic high-temperature compressive response has been experimentally investigated [6] earlier.

It has been very challenging to conduct high-temperature Kolsky tension bar experiments. The concept of cold contact time (CCT), which is commonly used in high-temperature Kolsky compression bar experiments, is no longer applicable to high-temperature Kolsky tension bars. In a Kolsky tension bar test, the specimen has to be firmly attached to the bar ends before heating and dynamic loading. In order to minimize the heat transfer from the high-temperature tensile specimen to the room-temperature pressure bars, Scapin et al. [7] applied a Cortex-tube-based air cooling system to cool down the bars while the specimen was heated up to $400 \text{ }^\circ\text{C}$. However, this air cooling system may not be sufficient for the experiments at higher temperatures, i.e., 750 and $1030 \text{ }^\circ\text{C}$, in this study. In addition, when characterizing thin sheet iridium specimens, special fixtures are needed. However, the complex specimen fixtures may modify the stress wave propagation. For instance, a stress wave reflection may be generated at each interface within the joints/fixtures between the specimen and the bars. In this case, the reflected wave, which is usually used to calculate the strain rate and strain in the specimen, is no longer reliable. Direct displacement measurements, i.e. non-contact optical measurements, on both ends of the specimen are required. The thermal expansion in the small and thin iridium tensile specimen may generate additional measurement issues that need to be properly addressed.

B. Song (✉) • R. Lipinski • J. Bignell
Sandia National Laboratories, Albuquerque, NM 87185, USA
e-mail: bsong@sandia.gov

K. Nelson
Sandia National Laboratories, Livermore, CA 94550, USA

G.B. Ulrich • E.P. George
Oak Ridge National Laboratory, Oak Ridge, TN 37831, USA

In this study, the conventional Kolsky tension bar was modified to characterize dynamic tensile stress–strain response of thin-sheet DOP-26 iridium alloy specimens at elevated temperatures. Specimens were characterized at two different strain rates (~ 1000 and 3000 s^{-1}) and temperatures (~ 750 and $1030 \text{ }^\circ\text{C}$) in order to determine the effects of strain rate and temperature on the tensile stress–strain response.

20.2 Modified High-Temperature Kolsky Tension Bar System

Figure 20.1a shows a schematic of the modified high-temperature Kolsky tension bar system and Fig. 20.1b–e show the detailed modifications for high-temperature experiments. A flat dog-bone shaped tensile specimen and corresponding fixture are shown in Fig. 20.1b. The fixture was machined with a slot with the same dimensions as the non-gage section of

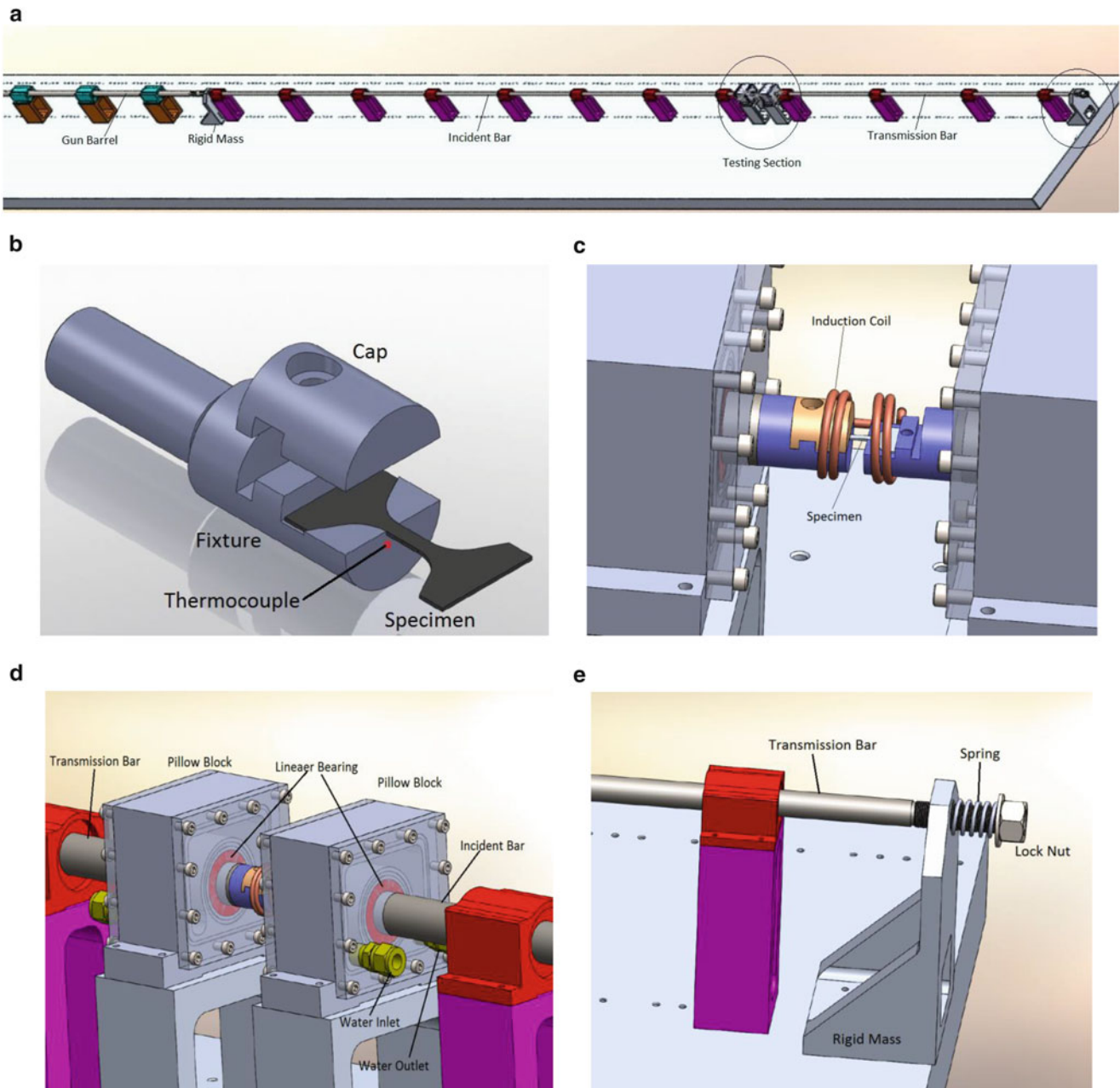


Fig. 20.1 Schematic of Kolsky tension bar with pulse shaping (a) Schematic of the modified high-temperature Kolsky bar system (b) Specimen fixture (c) Heating and testing section (d) Water cooling system (e) Spring-loaded pre-tension system

the specimen such that the whole non-gage section of the specimen was placed into the slot of the fixture. This design allows the load to be applied through the specimen shoulders to the gage section. The specimen was then covered with a semicircular cap. Both the fixtures and the semicircular caps were made of Inconel 718 steel, which has a relatively high strength at elevated temperatures. An induction coil heater was installed on the testing section, as shown in Fig. 20.2c. When the fixtures were heated with the induction coil, the heat was transferred to both the specimen and the bars simultaneously. In order to prevent heating of the bars, a pair of hollow water-cooled pillow blocks was installed on the bar ends, as shown in Fig. 20.2d. A splitting-beam laser extensometer presented in Ref. [8] was employed in this study to independently measure the displacements at both ends of the specimen. In this study, the laser detectors had been calibrated to exhibit a perfect linearity but with different factors: 0.732 mm/v at the incident bar side and 0.258 mm/v at the transmission bar side. The specimen strain can be calculated as

$$\varepsilon = \frac{L_1 - L_2}{L_s} \quad (20.1)$$

where L_1 and L_2 are displacements of the specimen ends attached to the incident and transmission bars, respectively; L_s is the gage length of the specimen. As shown in Fig. 20.1a, the non-gage sections of the specimen were enclosed in the fixtures. Equation (20.1) maximizes the representation of the actual deformation of the gage section without the need for correction with respect to the deformation in the non-gage sections.

A spring-loaded pre-tension system, as shown in Fig. 20.1e, was developed to prevent the specimen from buckling due to thermal expansion during heating. The spring was placed between a rigid mass and a flange (Fig. 20.1e). The flange was screwed toward the rigid mass to compress the spring, which in turn generated a tension load in the tension bar system including the tensile specimen. Another rigid mass was placed against the gun barrel (Fig. 20.1) to prevent the bar system from moving backwards when the whole bar system was pre-loaded in tension [9]. In this study, the spring was set to generate a pre-tension load of approximately 18 N which is sufficient to straighten the iridium specimen during heating but insufficient to produce further stretch on the iridium specimen.

Another high temperature testing issue is thermal softening of the specimen. A pair of semiconductor strain gages was used to replace the regular resistor strain gages on the transmission bar. The semiconductor strain gages had a gage factor of 139, which is approximately 70 times more sensitive than the regular resistor strain gages. The specimen stress is calculated as

$$\sigma = \frac{E_0 A_0 \varepsilon_t}{A_s} \quad (20.2)$$

where E_0 is Young's modulus of the bar material; A_0 is the cross-sectional area of the transmission bar; ε_t is the transmitted strain; and A_s is the cross-sectional area of the specimen. Combining the measurements of the semiconductor strain gages (20.2) and the laser system (20.1) for specimen stress and strain histories, respectively, yields the stress-strain curve of the specimen under investigation.

20.3 Dynamic High-Temperature Tensile Characterization of Iridium Alloy

The iridium tensile specimens were removed from prime DOP-26 alloy blanks using electrical discharge machining (EDM) with zinc-coated brass wire. The specimens were ground to remove the residual EDM layer, and then deburred and polished. All specimens were acid cleaned and then heat treated at 1375 ± 25 °C for $1 \text{ h} \pm 10 \text{ min}$ in vacuum (1×10^{-4} Torr). The tensile specimens had a thickness of 0.66 mm, a width of 2.54 mm, and a gage length of 6.35 mm. The detailed dimensions of the iridium specimens used in this study are shown in Fig. 20.2.

Figure 20.3 shows typical strain gage signals on the incident and transmission bars for the incident, reflected, and transmitted waves at the test temperature of 1030 °C. It is noted again that, the reflected pulse was not reliable and could not be used for specimen strain measurement. Instead, we used the laser system to directly track the movements of the specimen ends that were attached to the incident and transmission bars. The laser outputs shown in Fig. 20.4 clearly show significant change in the laser output for the front end (on the incident bar side) but no significant change for the back end (on the transmission bar side). This is because the transmitted force was too small to generate significant displacement on the transmission bar side.

Fig. 20.2 Iridium tensile specimen design (mm)

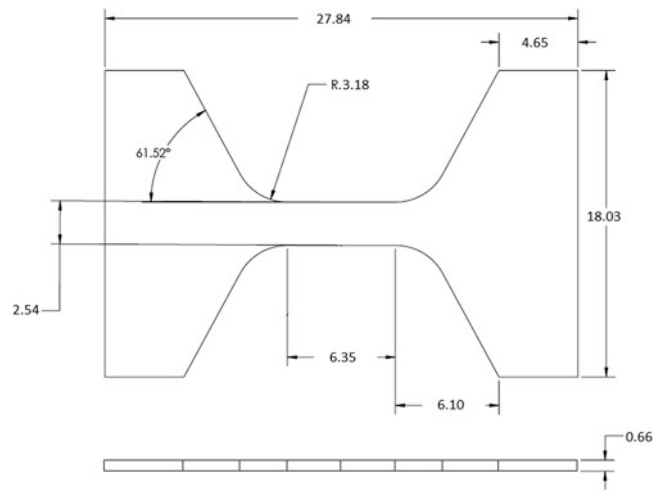


Fig. 20.3 Typical strain-gage signals

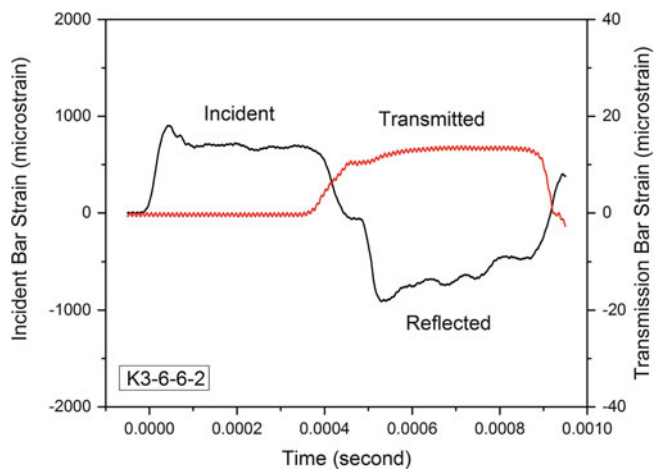
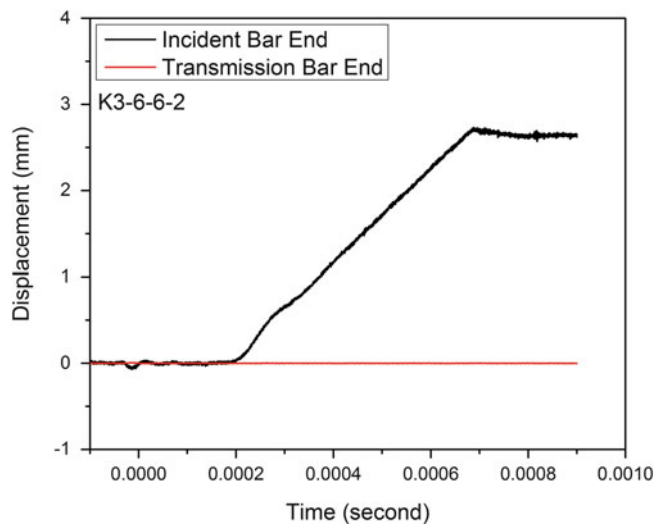


Fig. 20.4 Laser outputs



The engineering stress and strain histories in the specimen, which were calculated with (20.2) and (20.1), respectively, are shown in Fig. 20.5. The strain rate was then calculated with the slope of the strain history as a nearly constant 860 s^{-1} . The stress history exhibits oscillations because of the effect of the electromagnetic field generated by the induction coil on the highly-sensitive semiconductor strain gage signals. In this study, the raw data of stress history was filtered to remove

Fig. 20.5 Stress and strain histories

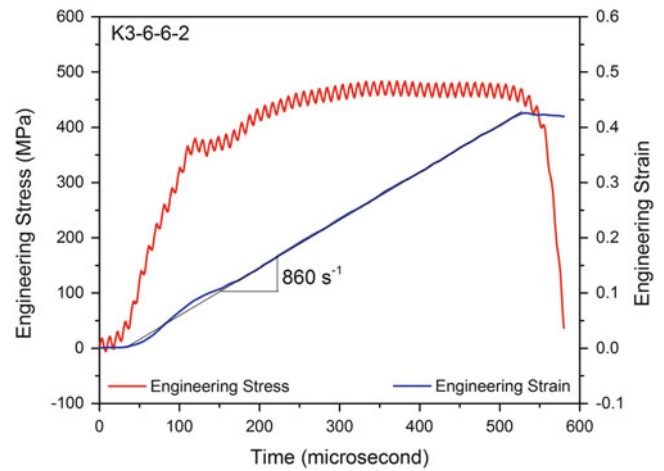
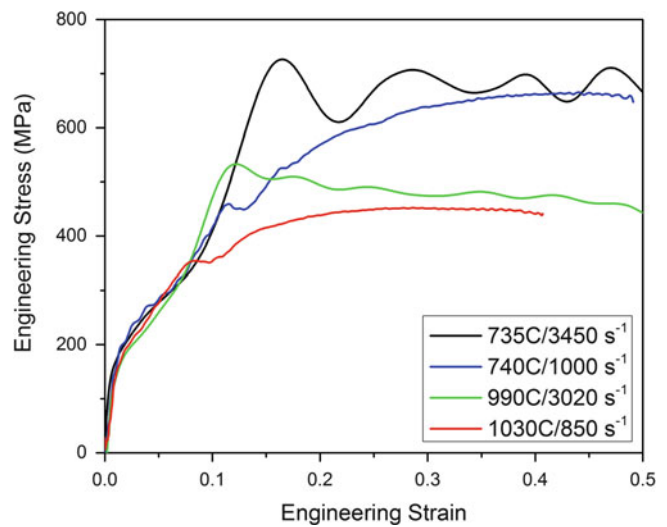


Fig. 20.6 Tensile stress–strain curves of iridium alloy at different strain rates and temperatures



the oscillations. Based on the stress and strain histories shown in Fig. 20.5, the tensile stress–strain curve at 860 s^{-1} and $1030 \text{ }^{\circ}\text{C}$ was obtained.

Following the same procedure, the iridium alloy was characterized in tension at two different strain rates (~ 1000 and 3000 s^{-1}) and temperatures (~ 750 and $1030 \text{ }^{\circ}\text{C}$). Three specimens were tested at each condition. The results were consistent (within 10 %) for each testing condition. Figure 20.6 shows the mean tensile stress–strain curves of the iridium alloy at different strain rates and temperatures. Due to the superior ductility of the iridium alloy at elevated temperatures, the specimens did not fail during the first dynamic tensile load except for the testing condition of $735 \text{ }^{\circ}\text{C}/3450 \text{ s}^{-1}$. At the $735 \text{ }^{\circ}\text{C}/3450 \text{ s}^{-1}$ condition, the engineering failure strains varied between 0.5 and 0.7. It is noted that the engineering failure strains were not representative of the actual failure strain since significant strain localization and necking occurred in the specimens before failure. Therefore, the stress–strain curves are plotted up to a strain of 0.5 in Fig. 20.6. The dynamic high-temperature stress–strain curves of the iridium alloy show different profiles than quasi-static curves [3]. All stress–strain curves show an initial elasticity followed by significant work hardening behavior when the strain is below 10 %. This phenomenon may be related to a change in microstructure or deformation mechanism at high strain rates and elevated temperatures. More oscillatory behavior was recorded in the stress–strain curve at $735 \text{ }^{\circ}\text{C}/3450 \text{ s}^{-1}$. The reason for this is still unknown and under investigation. When the strain is below 10 %, the stress–strain curves show neither strain-rate nor temperature effects. When the strain increases, the stress–strain curves show plastic flow with significant strain-rate and temperature effects. At strains greater than 10 % and similar strain rates the flow stresses decrease when the temperature increases from 750 to $1030 \text{ }^{\circ}\text{C}$, showing significant thermal-softening behavior. At the same temperature, the flow stresses increase when the strain rate increases from ~ 1000 to 3500 s^{-1} , showing a positive strain-rate sensitivity.

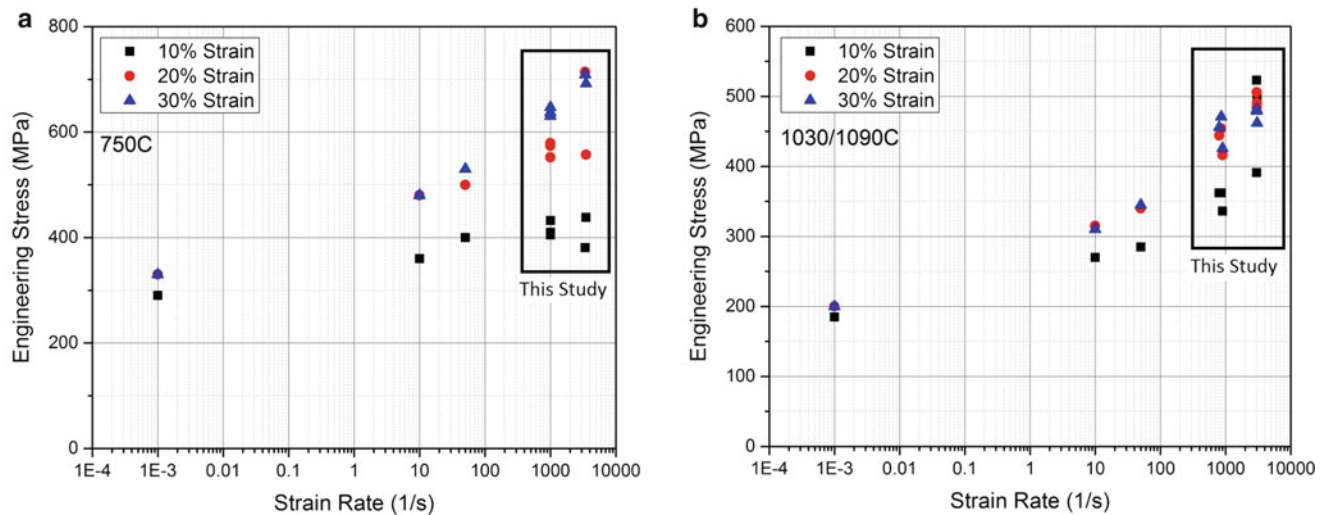


Fig. 20.7 Effect of strain rate on the tensile stress–strain response of iridium alloy at different temperatures (a) Strain rate effect at 750 °C (b) Strain rate effect at 1030/1090 °C

Figure 20.7 shows the detailed strain-rate effects including the quasi-static data at different strain rates and temperatures presented in [3]. The data obtained from this study are marked while the rest are from the reference [3] in both figures. Figure 20.7 clearly shows a significant strain-rate effect on the tensile flow stress of the iridium alloy at both temperatures. The strain-rate sensitivities are slightly different at the two temperatures and are also dependent on the level of strain.

20.4 Conclusions

The conventional direct-tension Kolsky bar was modified for high-temperature tensile characterization of the DOP-26 iridium alloy. An induction coil was applied to heat the iridium specimen to elevated temperatures up to 1030 °C while the specimen ends of the incident and transmission bars were cooled to reduce the thermal gradient in the bars. A pair of semiconductor strain gages on the transmission bar were used to directly measure the force/stress in the specimen during dynamic loading. A laser system was developed to independently measure the displacements at the specimen ends on the incident- and transmission-bar sides so that the specimen strain could be calculated. A spring-loaded pretension system was installed on the free end of the transmission bar to prevent the high-temperature specimen from buckling during heating. Dynamic tensile stress–strain curves of the iridium alloy were obtained at two temperatures (750 and 1030 °C) and strain rates (~ 1000 and 3000 s^{-1}). The iridium alloy shows high ductility at elevated temperatures and strain rates. The effects of strain rate and temperature on the tensile stress–strain response of the iridium alloy were also determined. The iridium alloy exhibits little sensitivity to strain rate or temperature when the strain is below 10 %, but strong sensitivities to both strain rate and temperature when the strain is greater than 10 %.

Acknowledgements The authors would like to acknowledge the support of Dr. Helena Jin for the preliminary DIC work and Kevin Connelly for his initial specimen and fixture design support.

This work was sponsored by the United States Department of Energy (DOE) Office of Space and Defense Power Systems (NE-75). The authors gratefully acknowledge the support and guidance of Ryan D. Bechtel of the US Department of Energy.

Sandia National Laboratories is a multi-program laboratory managed and operated by Sandia Corporation, a wholly owned subsidiary of Lockheed Martin Corporation, for the U.S. Department of Energy’s National Nuclear Security Administration under contract DE-AC04-94AL85000.

Oak Ridge National Laboratory is a multi-program research laboratory managed by UT-Battelle, LLC, for the US DOE under contract DE-AC05-00OR22725.

References

1. Ohriner, E.K.: Processing of iridium and iridium alloys, methods from purification to fabrication. *Platin. Met. Rev.* **52**, 186–197 (2008)
2. George, T.G.: High-strain-rate, high-temperature biaxial testing of DOP-26 iridium. Los Alamos National Laboratory Report, LA-11065 (1998)
3. Schneibel, J.H., Carmichael, C.A., George, E.P.: High strain rate tensile testing of DOP-26 iridium. Oak Ridge National Laboratory Report, ORNL/TM-2007/81 (2007). Oak Ridge National Laboratory
4. McKamey, C.G., George, E.P., Lee, E.H., Ohriner, E.K., Cohron, J.W.: Impurity effects on high-temperature tensile ductility of iridium alloys at high strain rate. *Scr. Mater.* **42**, 9–15 (2000)
5. George, E.P., Bei, H., Lee, E.H., Braden, J.D.: Tensile impact ductility and fracture behavior of DOP-26 iridium at 500–900 °C, Oak Ridge National Laboratory Report, ORNL/TM-2004/239 (2004)
6. Song, B., Nelson, K., Lipinski, R., Bignell, J., Ulrich, G., George, E.P.: Dynamic high-temperature testing of an iridium alloy in compression at high-strain rates. *Strain* **50**, 539–546 (2014)
7. Scapin, M., Peroni, L., Fichera, C.: Investigation of dynamic behaviour of copper at high temperature. *Mater. High Temp.* **31**, 131–140 (2014)
8. Nie, X., Song, B., Loeffler, C.M.: A novel splitting-beam laser extensometer technique for Kolsky tension bar experiment. *J. Dyn. Behav. Mater.* **1**(1), 70–74 (2015)
9. Song, B., Lu, W.-Y.: Preload high-rate tension techniques. In *Proceedings of SEM XII International Congress and Exposition on Experimental and Applied Mechanics*, Costa Mesa, (2012)